Korean J. Chem. Eng., **30**(12), 2248-2253 (2013)
DOI: 10.1007/s11814-013-0164-y

pISSN: 0256-1115
eISSN: 1975-7220

Experimental and theoretical investigations on the carbon dioxide gas hydrate formation kinetics at the onset of turbidity regarding CO_2 capture and sequestration processes

Bahman ZareNezhad†, Mona Mottahedin, and Farshad Varaminian

School of Chemical, Petroleum and Gas Engineering, Semnan University, P. O. Box 35195-363, Semnan, Iran
(*Received 23 July 2013 • accepted 27 August 2013*)

Abstract−The carbon dioxide gas hydrate formation kinetics at the onset of turbidity is experimentally and theoretically investigated. It is shown that the time-dependent heterogeneous nucleation and growth kinetics are simultaneously governing the hydrate formation process at the onset of turbidity. A new approach is also presented for determination of gas hydrate-liquid interfacial tension. The CO_2 hydrate-liquid interfacial tension according to the suggested heterogeneous nucleation mechanism is found to be about 12.7 mJ/m^2. The overall average absolute deviation between predicted and measured CO_2 molar consumption is about 0.61%, indicating the excellent accuracy of the proposed model for studying the hydrate-based CO_2 capture and sequestration processes over wide ranges of pressures and temperatures.

Key words: CO_2, Sequestration, Energy, Nucleation, Growth, Interfacial Tension, Gas Hydrate, Kinetics

INTRODUCTION

Capture and disposal of CO_2 is actively being sought as a means to avoid release of greenhouse gases to the atmosphere [1-3]. With the reality of increasing fossil fuel use, focus should be aimed at developing and establishing promising energy management systems that can prevent release of CO_2 to the atmosphere [4-6]. This must be aggressively pursued with the impetus of increasingly stringent carbon restrictions and problems associated with global warming. Hydrate technology offers a possible alternative for capturing and disposal of carbon dioxide [7,8]. In this technology the waste CO_2 from large point sources such as fossil fuel power plants is captured and transported to a storage site and deposited in an underground geological formation [9,10].

A commercially viable hydrate-based CO_2 separation process demands a rapid hydrate formation rate. Higher solubility of hydrate forming guest in water and larger contact area between the hydrate formers and water are very important [11,12]. These two factors reduce the mass transfer resistance, resulting in faster hydrate formation rate. Therefore, investigating the kinetics of gas hydrate formation is essential for the design of hydrate formation reactors at industrial scale [13,14].

In the process of hydrate crystallization, stable hydrate nuclei are generated from a supersaturated solution and grow continuously to form the hydrate crystals. Englezos et al. [15] developed a model based on crystallization and mass transfer effects for determination of methane and ethane gas hydrate kinetics. However, ZareNezhad et al. [16] have shown that the hydrate nucleation process in practical situations is a heterogeneous process, as homogeneity is rarely achieved. Recently, ZareNezhad et al. [17] also presented a new mechanistic model for description of CO_2 gas hydrate formation regarding carbon dioxide sequestration processes considering both growth kinetics and secondary nucleation kinetics for the first time.

The correct definition of driving force is quite important in hydrate nucleation study. Skovborg et al. [18] defined the driving force in terms of chemical potential difference for water. Natarajan et al. [19] defined driving force based on a fugacity difference for the guest molecule. Another definition frequently adopted is the degree of supercooling, that is, the difference between the operating temperature and the equilibrium temperature for hydrate formation. It can be demonstrated that these three forms are in fact particular cases of a more general driving force expressed by the variation in the Gibbs free energy of the system [7]. Kashchiev and Firoozabadi extended this approach and presented a new definition of driving force (supersaturation) for studying the gas hydrate nucleation kinetics [20,21].

The present study extends the Kashchiev and Firoozabadi nucleation model [22] to the onset of growth process. Kinetics of CO_2 hydrate formation during the nucleation period and early stage of hydrate growth processes is experimentally and theoretically investigated in a stirred jacketed reactor. A new technique is then introduced for accurate determination of high pressure gas hydrate-liquid interfacial tension required for design of CO_2 hydrate storage and sequestration equipments regarding newly developed energy management systems.

EXPERIMENTAL PROCEDURE

Carbon dioxide with a normal purity of 99.8%, supplied by a technical gas service, and distilled deionized water have been used in all experiments. The experiments were carried out in a 600 cm^3 stirred jacketed batch reactor equipped with a data acquisition system as shown in Fig. 1. The cell pressure was measured by a pressure transmitter with the accuracy of about ±0.01 MPa and the temperature was measured with accuracy of ±0.1 K. The signals of pressures and temperatures were acquired by a data logging system and recorded in a personal computer. The temperature of reactor was controlled by the flow of tri-ethylene glycol solution through the jacket.

After washing and rinsing the reactor with de-ionized water, the

†To whom correspondence should be addressed.
E-mail: prof.b.zarenezhad@gmail.com

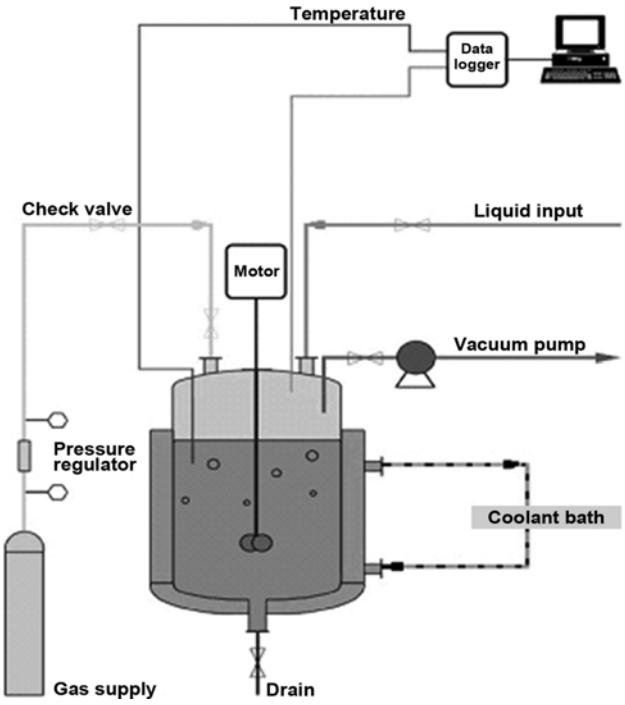

Fig. 1. Schematic diagram of gas hydrate formation system.

vessel was evacuated and then 300 cm^3 of distilled water was charged to the vessel. The cooling system was turned on and the reactor was allowed to reach the desired constant temperature. When the thermal equilibrium was maintained, the reactor was pressurized to the desired pressure by supplying gas from the cylinder. The magnet drive mixer was then turned on and the data logging system was started until the hydrate formation process was completed.

PROCESS MODELING

The rate of gas consumption at the early stage of hydrate crystallization can be written as [16,22]:

$$R(t)=\frac{dn(t)}{dt}=\left[\frac{b\rho_h V_s G^{3m} J}{M_h}\right]t^{3m} \tag{1}$$

where R(t) is the rate of gas consumption for a pure component in simple gas hydrate formation, ρ_h is hydrate density, V_s is the molar mass of the solution, M_h is the molecular weight of hydrate, b is the dimensionless shape factor, G and J are the growth and nucleation rates, respectively. For growth by volume diffusion of dissolved gas toward a spherical crystallite, m=1/2 and the growth rate, G, is defined by:

$$G=Q\left[e^{\left[\left(\frac{\Delta\mu}{kT}\right)\right]}-1\right] \tag{2}$$

where Q is the supersaturation-independent kinetic factor given by following equation:

$$Q=(2\varepsilon v_h D_{ef} C_e) \tag{3}$$

and C_e is the equilibrium solubility of gas component, $\varepsilon \leq 1$ is the sticking coefficient of building units to the crystallite surface. v_h is the volume of a hydrate building unit, D_{ef} is an effective diffusion coefficient characterizing the random events of transfer of hydrate building units across the nucleus/solution interface. Nucleation rate is determined by following formula:

$$J=A\exp\left[\frac{\Delta\mu}{kT}\right]\exp\left[\frac{-4c^3V_h^2\sigma_{ef}^3}{27kT\Delta\mu^2}\right] \tag{4}$$

where

$$A=\frac{z\varepsilon(4\pi c)^{\frac{1}{2}}V_h^{\frac{1}{3}}D_{ef}C_e\dot{n}^{\frac{1}{3}}}{A_w} \tag{5}$$

In the above equation, z is the Zeldovich factor and is determined by Eq. (6) [21]:

$$z=\sqrt{\frac{W}{3\pi kT\dot{n}^2}} \tag{6}$$

W is the work of cluster formation and $\dot{n}$ is the number of building units constituting a nucleus which is calculated by:

$$\dot{n}=\frac{8c^3V_h^2\sigma_{ef}^3}{27\Delta\mu^3} \tag{7}$$

A_w is the surface area of water molecule and c is the numerical shape factor equal to $(36\pi)^{1/3}$. The parameter σ_{ef} (J/m^2) is an effective specific surface energy (interfacial tension) of hydrate/solution interface. The supersaturation ($\Delta\mu$) in Eqs. (2) and (4) is expressed by [16,20]:

$$\Delta\mu=kT\left[\frac{\varphi(P,T)P}{\varphi(P_e,T)P_e}\right]+\Delta V_e(P-P_e) \tag{8}$$

Such that

$$\Delta V_e=n_w(P_e,T).V_w(P_e,T)-V_h(P_e,T) \tag{9}$$

where ΔV_e is the difference between the volume of n_w water molecules in the solution and volume of hydrate building unit in crystal, k is the Boltzmann constant, P_e is the hydrate equilibrium pressure at T, ϕ and ϕ_e are the fugacity coefficients of gas at given P and T and P_e and T, respectively. In the current study, Fugacity coefficients were determined by using the Peng-Robinson equation of state [23].

Experiments of carbon dioxide hydrate formation were performed at isothermal-isochoric operating conditions. During the induction time, system pressure remains constant so the nucleation and growth rates are time independent parameters, but at the end of induction period, the nucleation rate decreases sharply as the supersaturation declines. In the present work it is assumed that at early stage of growth process, the heterogeneous nucleation is still governing the process. The time dependent nucleation and growth rates are incorporated in the model by integrating Eq. (1) in combination with Eqs. (2)-(9) over initial growth period using the Runge-Kutta-Fehlberg numerical technique with the time step of 0.01 s.

RESULTS AND DISCUSSION

The variation of carbon dioxide molar consumption during hydrate formation at three different impeller speeds of 400, 600 and 800 RPM at 274.15 K is shown in Fig. 2. It is quite clear that at an im-

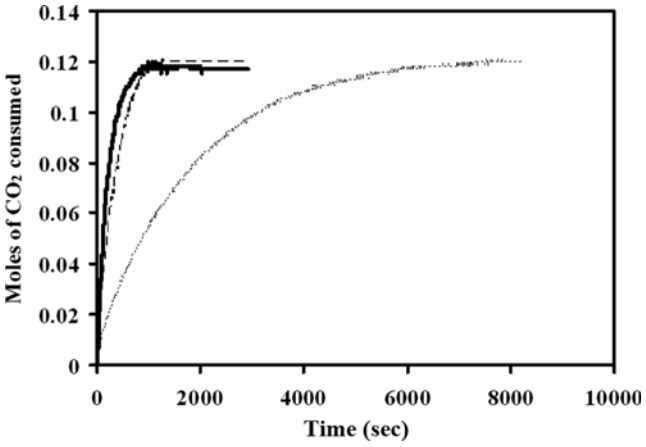

Fig. 2. Comparison the rate of hydrate formation at three different impeller speeds (····· 400 RPM, —— 600 RPM, ——— 800 RPM).

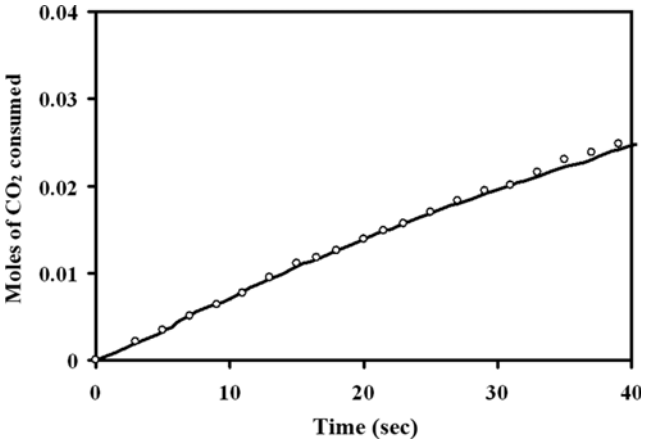

Fig. 3. Moles of carbon dioxide consumed during hydrate formation at 274.15 K and initial pressure of 2.01 MPa (— calculated, ○ experimental).

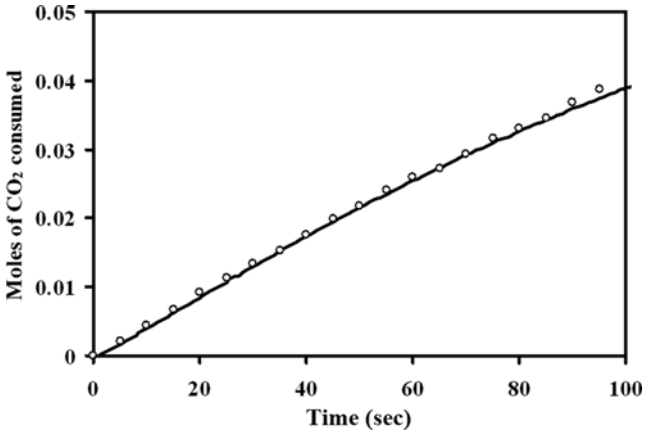

Fig. 4. Moles of carbon dioxide consumed during hydrate formation at 275.15 K and initial pressure of 2.2 MPa (— calculated, ○ experimental).

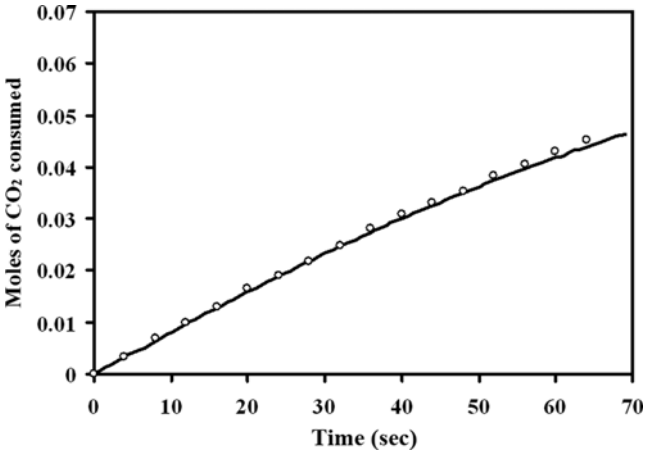

Fig. 5. Moles of carbon dioxide consumed during hydrate formation at 276.15 K and initial pressure of 2.41 MPa (— calculated, ○ experimental).

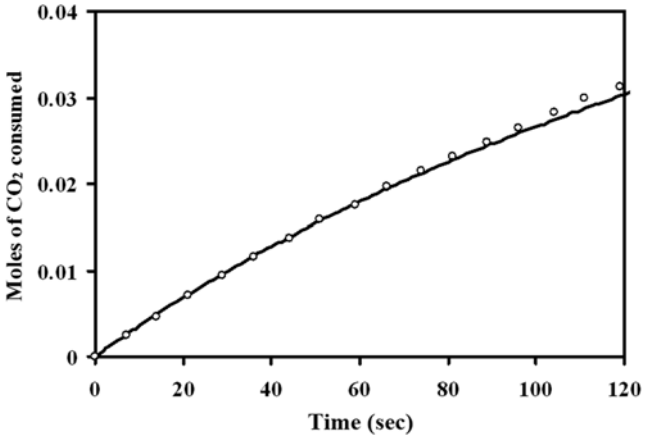

Fig. 6. Moles of carbon dioxide consumed during hydrate formation at 277.15 K and initial pressure of 2.52 MPa (— calculated, ○ experimental).

peller speed above 600 RPM, the system becomes fully agitated such that by increasing the impeller speed to 800 RPM, a very small change in the molar consumption profiles is observed. At such an operating condition, the mass transfer resistance at the gas-liquid interface is negligible and the kinetics of hydrate formation can be accurately determined at nearly homogeneous condition. Therefore, in the present study, the experimental data at the impeller speed of 800 RPM were collected and used for determination of CO_2 hydrate kinetics and hydrate-liquid interfacial tension at different temperatures and pressure driving forces.

Comparison of the predicted and measured molar consumption of CO_2 gas at the early stage of gas hydrate formation process at different operating temperatures is shown in Figs. 3-7. In all figures, the time t=0 is the commencement of solution turbidity. Since at higher initial pressures the temperature rising at the onset of hydrate formation is more sensible, we tried hard to keep the solution temperature at isothermal conditions by using an efficient control system. This is especially important when the system is operating at higher temperatures. An increase in system temperature leads to an increase in the equilibrium dissociation pressure of CO_2 hydrate. Thus depending on the employed temperature, the initial pressure has been adjusted proportionally to maintain a constant driving force in

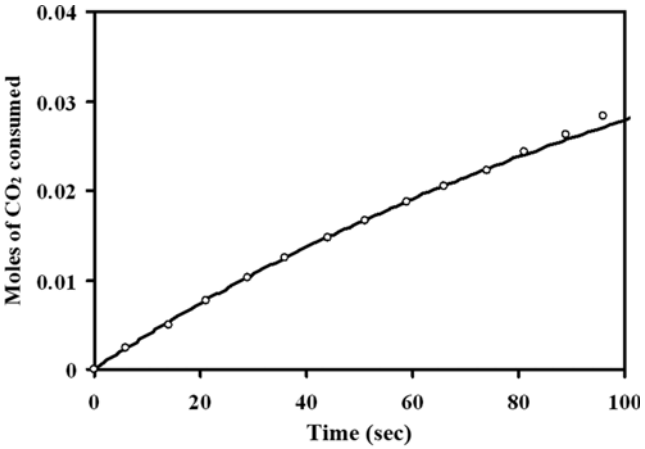

Fig. 7. Moles of carbon dioxide consumed during hydrate formation at 278.15 K and initial pressure of 2.6 MPa (— calculated, ○ experimental).

all experiments. According to Figs. 3-7, the predicted results are in excellent agreement with experimental data over the temperature range of 274.15-278.15 K. Considering the foregoing experimental difficulties, the presented approach has been employed successfully to describe the process.

All investigators have assumed that there is not any primary nucleation at the early stage of gas hydrate growth. However, the agreement of theoretical predictions with the measured data points in Figs. 3-7 suggests that both heterogeneous primary nucleation and growth kinetics are simultaneously governing the hydrate formation process at the onset of turbidity and thereafter up to at least 60 to 120 seconds, which is quite interesting. This phenomenon has never been reported previously in the available scientific literature regarding gas hydrates.

In aqueous phase the solubility of CO_2 is relatively high and the system approaches to the supersaturation state very quickly leading to a short induction time. For such a case, it is usually difficult to obtain accurate predictions, especially at the onset of hydrate growth. The presented approach has been used successfully for prediction of gas consumption profiles during gas hydrate formation over time domain when both heterogeneous nucleation and growth processes are influencing.

The presented approach can also be used for accurate determination of CO_2 hydrate-liquid interfacial tension, σ_{ef}. The optimum value of σ_{ef} is also determined by minimizing the deviations between predicted and experimental molar gas consumption rates at the early stages of hydrate growth process according to the following objective function:

$$\varepsilon_{\sigma_{ef}} = \sqrt{\sum_{i=1}^{ND} \frac{[R(t)_{pred.} - R(t)_{exp.}]^2}{ND}} \quad (10)$$

The predicted σ_{ef} according to Eq. (10) is found to be much more reliable as compared to the conventional method which employs scattered and inaccurate induction time data [22].

The calculated values of σ_{ef} regarding different experimental runs are presented in Table 1 and compared in Fig. 8. Interestingly, the calculated CO_2 hydrate-liquid interfacial tensions are very close together with the average value of 12.7 mJ/m^2 regardless of operating temperatures and pressures. Note that measurement of σ_{ef} by

Table 1. Calculated values of and AAD% at different operating conditions according to the proposed technique in the present work

Run number	Temperature (K)	Initial pressure (MPa)	Impeller speed (RPM)	σ_{ef} (mJ/m^2)	AAD%
R1	274.15	2.01	800	12.56	0.64
R2	275.15	2.2	800	12.73	0.58
R3	276.15	2.41	800	12.28	0.53
R4	277.15	2.52	800	12.97	0.66
R5	278.15	2.6	800	12.95	0.68
R6	278.65	2.7	800	12.70	0.57

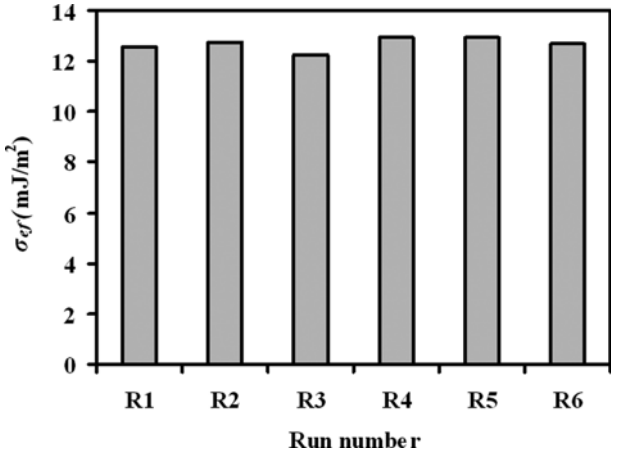

Fig. 8. The calculated values of CO_2 hydrate-liquid interfacial tension at different operating conditions.

conventional method according to the scattered induction time data is not accurate, especially for the case of highly soluble CO_2 where the supersaturation state is quickly approached and the induction time is too short to be employed for reliable determination of hydrate-liquid interfacial tensions. That is why most investigators have used a σ_{ef} of about 20 mJ/m^2 according to the classical homogeneous nucleation [22]. However, we have recently shown [16] that heterogeneous nucleation is usually the dominant mechanism at the onset of gas hydrate formation processes. The thermodynamic approach which has been employed by some investigators [24,25] for determination of CO_2 hydrate-water interfacial tension in porous media leads to different inconsistent results because of different geometric assumptions. The value obtained by Uchida et al. [24] is 14±3 mJ/m^2, which is about half of that obtained by Anderson et al. [25]. We believe that the estimated σ_{ef} value of about 12.7 mJ/m^2, according to the proposed technique in the present work, is quite reliable for accurate design of hydrate based-CO_2 sequestration systems.

The predicted and measured CO_2 molar consumptions at the onset of turbidity and early stage of gas hydrate formation at different operating pressures, temperatures and driving forces are compared in Fig. 9. The prediction accuracy is evaluated by determination of average absolute deviation according to the following equation:

$$AAD\% = \frac{1}{ND}\sum_{i=1}^{ND} \frac{|n_{i,calc} - n_{i,exp}|}{n_{i,exp}} \times 100 \quad (11)$$

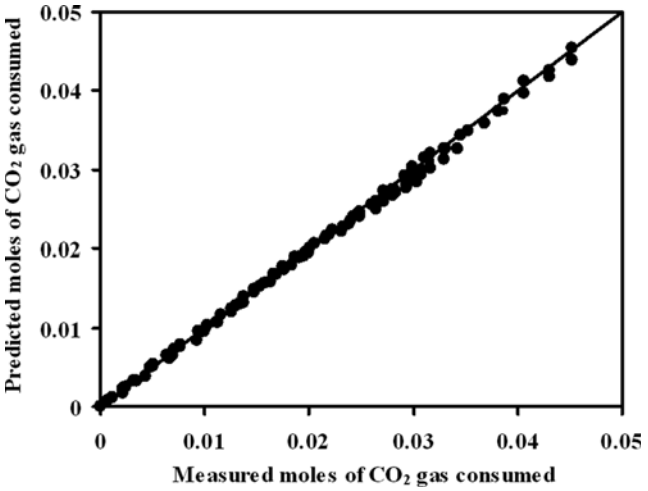

Fig. 9. Comparison of predicted and measured CO_2 molar consumption regarding onset of gas hydrate formation.

where $n_{i,cal}$ and $n_{i,exp}$ are the predicted and measured moles of CO_2 consumed respectively and ND is the number of data points. The overall AAD% of the predicted results considering all experimental runs is about 0.61% as shown in Table 1, and overall R^2-value regarding all data points according to Fig. 9 is about 0.988, indicating the excellent accuracy of the proposed approach over wide ranges of pressures and temperatures.

CONCLUSIONS

Carbon dioxide gas hydrate formation kinetics at the onset of turbidity regarding CO_2 capture and sequestration processes is experimentally and theoretically investigated. A theoretical framework has been proposed for prediction of gas consumption profiles during gas hydrate formation at the onset of turbidity when both heterogeneous nucleation and growth processes are influencing. A new approach has also been employed for accurate determination of CO_2 hydrate-liquid interfacial tension by minimizing the deviations between predicted and experimental molar gas consumption rates at the early stages of hydrate growth process. The presented technique is an accurate alternative to the unreliable induction time measurement method, especially for the case of highly soluble gas hydrate formers where the supersaturation state is quickly approached. The overall average absolute deviation between predicted and measured moles of consumed CO_2 at the onset of turbidity is about 0.61%, indicating the accuracy of the presented model over wide ranges of operating conditions. The proposed technique is quite useful for evaluating the effects of different variables on the process kinetics, especially at the initial period of gas hydrate formation when both nucleation and growth processes are influencing.

NOMENCALTURE

AAD% : average absolute deviation percent
A : kinetic parameter for pure gas hydrate formation [m^{-3} s^{-1}]
A_w : surface area of water molecule [m^2]
b : dimensionless shape factor
c : numerical shape factor
C_e : equilibrium solubility of gas component [m^{-3}]
D_c : gas diffusivity in the aqueous solution [m^2 s^{-1}]
f : fugacity [Pa mol^{-1} m^3]
G : growth rate [m^2 s^{-1}]
J(t) : nucleation rate [m^{-3} s^{-1}]
k : Boltzmann constant [J K^{-1}]
M : molar mass [g mol^{-1}]
ND : number of data points
N_w : number of water molecule per unit cell
N_{ava} : Avogadro number [mol^{-1}]
$n_{i,cal}$: predicted moles of CO_2 consumed at instant i
$n_{i,exp}$: measured moles of CO_2 consumed at instant i
$\dot{n}$: amount of building units constituting a nucleus
n_w : hydration number
P : pressure [MPa]
P_e : equilibrium pressure [MPa]
Q : supersaturation- independent kinetic factor [m s^{-1}]
R : universal gas constant [J mol^{-1} K^{-1}]
R(t) : rate of gas consumption for pure component [mol s^{-1}]
T : absolute temperature of system [K]
t : time [s]
V_s : initial volume of solution [m^3]
W : work of cluster formation [J]
z : Zeldovich factor

Greek Symbols

ρ_h : hydrate density [Kg m^{-3}]
ε : the sticking coefficient of building units to the crystallite surface
$\varepsilon_{\sigma_{eff}}$: error criterion in Eq. (10)
σ_{ef} : effective surface energy [J m^{-2}]
ϕ : fugacity coefficient of gas at P and T
$\Delta\mu$: supersaturation or driving force of hydrate formation [J]
ΔV_e : difference between the volume of n_w water molecules in the solution and the volume of a hydrate building unit in the hydrate crystal at the equilibrium pressure

REFERENCES

1. D. Aaron and C. Tsouris, *Sep. Sci. Technol*., **40**, 321 (2005).
2. P. Englezos and J. D. Lee, *Korean J. Chem. Eng*., **22**, 671 (2005).
3. P. Linga, R. Kumar and P. Englezos, *J. Hazard. Mater*., **149**, 625 (2007).
4. S. M. Klara and R. D. Srivastava, *Environ. Prog*., **21**, 247 (2002).
5. S. P. Kang, H. Lee, *Environ. Sci. Technol*., **34**, 4397 (2000).
6. N. H. Duc, F. Chauvy and J. M. Herri, *Energy Convers. Manage.*, **48**, 1313 (2007).
7. E. D. Sloan and C. A. Koh, *Clathrate hydrates of natural gases*, 3rd Ed. New York, CRC Press (2008).
8. G. Li, D. Liu, Y. Xie and Y. Xiao, *Energy Fuel*, **24**, 4590 (2010).
9. J. B. Klauda and S. I. Sandler, *Energy Fuel*, **19**, 459 (2005).
10. Y. F. Makogon, S. A. Holditch and T. Y. Makogon, *J. Petrol. Sci. Eng.*, **56**, 14 (2007).
11. H. Tajima, A. Yamasaki and F. Kiyono, *Energy*, **29**, 1713 (2004).
12. P. Linga, R. Kumar and P. Englezos, *Chem. Eng. Sci.*, **62**, 4268 (2007).
13. H. J. Lee, J. D. Lee, P. Linga, P. Englezos, Y. S. Kim and M. S. Lee,

Energy, **35**, 2729 (2010).
14. X. S. Li, C. G. Xu, Z. Y. Chen and H. J Wu, *Energy*, **35**, 3902 (2010).
15. P. Englezos, N. Kalogerakis, P. D. Dholabhai and P. R. Bishnoi, *Chem. Eng. Sci*., **42**, 2647 (1987).
16. B. ZareNezhad, M. Mottahedin and F. Varaminian, *The Assessment of Nucleation Kinetic Mechanisms in Gas Hydrate Crystallization Processes*, submitted for publication in *Korean J. Chem. Eng.* (2013).
17. B. ZareNezhad and M. Mottahedin, *Energy Convers. Manage.*, **53**, 332 (2012).
18. P. Skovborg and P. Rasmussen, *Chem. Eng. Sci*., **49**, 1131 (1994).
19. V. Natarajan, P. R. Bishnoi and K. Kalogerakis, *Chem. Eng. Sci*., **49**, 2957 (1994).
20. D. Kashchiev and A. Firoozabadi, *J. Crystal Growth*, **241**, 220 (2002).
21. D. Kashchiev and A. Firoozabadi, *J. Crystal Growth*, **243**, 476 (2002).
22. D. Kashchiev and A. Firoozabadi, *J. Crystal Growth*, **250**, 499 (2003).
23. D. Y. Peng and D. B. Rabinsom, *Ind. Eng. Chem. Fund*., **15**, 59 (1976).
24. T. Uchida, T. Ebinuma, S. Takeya, J. Nagao and H. Narita, *J. Phys. Chem., B*, **106**, 820 (2002).
25. R. Anderson, M. Llamedo, B. Tohidi and R. W. Burgass, *J. Phys. Chem., B*, **107**, 3507 (2003).